# Development of Fluorescent Immunochromatographic Test Strip for Qualitative and Quantitative Detection of Zearalenone

Qingbao Yang[1] · Yanhua Qi[1] · Jingming Zhou[1] · Hongliang Liu[1] · Yankai Liu[1] · Yumei Chen[1] · Chao Liang[1] · Aiping Wang[1]

## Abstract

Zearalenone (ZEN), which is usually generated by *Fusarium* species, is common contamination of corn. ZEN induces estrogen effects and disrupts the reproductive system of humans and animals. Herein, we established a method of quantum dots (QDs) immunochromatographic test strips for the detection of ZEN. In this method, QDs (Q2605, G2701A) and anti-ZEN monoclonal antibodies were conjugated by carbodiimide. The control line and test line of test strips were sprayed with staphylococcal protein A and ZEN-BSA, respectively. The standard curve equation of quantitative detection was $y = 0.3958x + 0.3233$ ($R^2 = 0.9914$). The limit of detection and 50% comparative inhibition ($IC_{50}$) were 0.273 ng/mL and 2.792 ng/mL, respectively. The test strips showed a linear range of detection (0.488–15.996 ng/mL). In the intra-assay, recovery ranged from 85.62 to 98.57% and the coefficient of variation (CV) was less than 5.53%. In the inter-assay, it ranged from 84.43 to 100.54% with a CV lower than 8.79%. Briefly, the test strips were established and could be used as a rapid and sensitive method for the detection of ZEN in corn.

**Keywords** Fluorescent · Immunochromatographic test strip · Quantum dots · Zearalenone

## Introduction

Zearalenone (ZEN) is a common mycotoxin produced by *Fusarium* species. ZEN is listed as a group III carcinogen by the International Agency for Research on Cancer (IARC) (Zhang et al. 2017). It usually contaminates corn, wheat, rice, cereals, and soybeans (Luo et al. 2018; Alshannaq and Yu 2017). ZEN increases the risk of cancer in humans and animals due to the ingestion of contaminated food (Chen et al. 2019; Zhang et al. 2017). Furthermore, ZEN can induce estrogen effects and disrupt the reproductive system of humans and animals (Massart et al. 2008; Krska and Josephs 2001). Thus, it is critical to monitor and control ZEN residues in corn. European Union (EU) and China have set the maximum level (ML) of mycotoxins contaminants in foodstuffs (Sun et al. 2016). The MLs of ZEN for corn in the EU and China are 100 μg/kg and 60 μg/kg, respectively (Zhang et al. 2017; Xu et al. 2021). To control and monitor the level of ZEN in corn, it is necessary to establish a sensitive and easy-using method for its qualitative and quantitative detection.

Currently, various methods for the detection of ZEN have been developed to reduce its health risks (Shao et al. 2018). Enzyme-linked immunosorbent assay (ELISA) is widely applied in the detection of ZEN because of its simplicity and low cost (Cha et al. 2012; Thongrussamee et al. 2008). High-performance liquid chromatography coupled with tandem mass spectrometry (HPLC/MS) meets the requirements for highly sensitive identification of ZEN (Zhang et al. 2016; Zhao et al. 2017). An aptamer-based assay is also applied in the detection of ZEN using fluorescence resonance energy transfer effect (FRET) and fluorimetry (Wu et al. 2019). As a device of point-of-care testing (POCT), the immunochromatographic test strip has been frequently reported in the detection of mycotoxin (Zhang et al. 2011; Liu et al. 2020). Moreover, the immunochromatographic test strip has been widely applied in food safety and clinical analysis because of its rapidity, sensitivity, and accuracy (Sajid et al. 2015; Huang et al. 2016; Mahmoudi et al. 2019).

Previous research mainly focused on colloidal gold (CG)-based immunochromatographic test strip for the detection of

✉ Aiping Wang
  pingaw@126.com

1  School of Life Sciences, Zhengzhou University,
   Zhengzhou 450001, China

ZEN (Sun et al. 2016; Kolosova et al. 2007). The coupling of CG and monoclonal antibodies (mAb) is based on electrostatic adsorption, while quantum dots (QDs) coupling with mAb are based on covalent bonding. So, the stability of CG-mAb is lower than QDs-mAb, and the fluorescence of QDs is easier to be distinguished than CG (Foubert et al. 2017). To improve the sensitivity of immunochromatographic test strip, the QDs were mainly selected as the label of the fluorescent probe (Li et al. 2019). QD-based immunochromatographic test strip consumes less immunoreagents and is more sensitive than the CG-based immunochromatographic test strip (Wang et al. 2017; Beloglazova et al. 2011). Hence, QDs have been widely applied in sensors and electronics because of its stability and photoluminescence brightness (Gao et al. 2002; Ugarte et al. 2012). However, previous reports focused on using anti-mouse IgG or biotin-streptavidin system as the signal output of the QD immunochromatographic test strip (Wu et al. 2019; Shao et al. 2019). There are few reports on using staphylococcal protein A (SPA) instead of anti-mouse IgG as a quality control line of the QD immunochromatographic test strip. As a broad-spectrum secondary antibody, SPA is easy to prepare and purify and has a strong binding force with crystalline fragment (Fc) of IgG. Antigen-binding fragment (Fab) of IgG extends outward after the combination of SPA and the Fc region, which improves the ability of the quality control line to fix antibodies and the efficiency of antigen–antibody binding (Wang et al. 2019a; Zhang et al. 2013). This is conducive to the better color development of the immunochromatographic test strip.

In this study, CdSe/ZnS QDs were used to prepare fluorescent probes, and SPA was sprayed on the control line of test strips for qualitative and quantitative detection of ZEN in corn. The developed test strips provided a useful method for the detection of mycotoxin contamination in food. This was good for both human health and environmental pollution intervention. As a promising point-of-care testing (POCT) device, the test strips improved the detection efficiency and reduced the risk of ZEN contamination in food.

## Materials and Methods

### Materials

Water-soluble QDs (Q2605, G2701A) were provided by Jiayuan Quantum Dots Co., Ltd. (Wuhan, China). Staphylococcal protein A (SPA) was obtained from Solarbio Science & Technology Co., Ltd. (Beijing, China). The 4D7 mAb against ZEN was previously produced in Henan Provincial Key Laboratory of Immunobiology (Zhou et al. 2021a). ZEN, Ochratoxin A (OTA), deoxynivalenol (DON), and T-2 toxin were purchased from

Pribolab Pte. Ltd. (Singapore). Bovine serum albumin (BSA), 1-(3-dimethylaminopropyl)-3-ethylcarbodiimide hydrochloride (EDC), $NaN_3$, nitrocellulose membrane, and ovalbumin (OVA) were purchased from Merck KGaA (Darmstadt, Germany). Trehalose was purchased from Beyotime Biotechnology (Shanghai, China). Tween-20 and acetonitrile were purchased from Zhiyuan Chemical Reagent Co., Ltd. (Tianjin, China). Phosphate-buffered saline (PBS) was prepared in our laboratory. Glass fiber, plastic cassette, and absorbent paper were purchased from Kinbio Tech. Co., Ltd. (Shanghai, China). The ultrapure water system instrument was obtained from a Thermo Scientific Nanopure Water Purifier (Waltham, USA).

### Instruments

The Dispense Platform (XYZ3050) and Guillotine Cutter (CM4000) were obtained from BioDot, Inc. (USA). The Centrifuge 5810 R was obtained from Eppendorf (Hamburg, Germany). The Nanodrop 2000c Spectrophotometer, drying oven, and ultrapure water system instrument were obtained from Thermo Scientific (Waltham, USA). The SpectraMax i3X microplate reader was purchased from Molecular Devices (USA). The multi-channel fluorescence immunoassay analyzer was obtained from Micro detection Co., Ltd. (Nanjing, China). The UV lamp with an excitation wavelength of 365 nm and incubator shaker was purchased from Crystal Technology & Industries, Inc. (CTI, USA). The nucleic acid-protein electrophoresis system was provided by Bio-Rad Laboratories, Inc. (USA). The homogenizer S1-M81 was obtained from Joyoung Co., Ltd. (Shandong, China).

### Bioconjugation QDs with Anti-ZEN mAb

The fluorescent probes (anti-ZEN mAb-QDs) were prepared according to previous research (Taranova et al. 2015). Briefly, 50 uL QDs (8 uM) were activated by EDC (9.563 μL, 1.0 mg/mL). They were blended and stirred with continuous shaking for 30 min. At this time, the carboxyl groups of QDs were activated. Subsequently, the anti-ZEN mAb (51.724 μL, 2.9 mg/mL) reacted with the QDs for 2.5 h. The amino group on mAb was combined with the carboxyl group on the QD through an amide bond (Fig. 1a). Afterward, a BSA solution was added and obstructed additional carboxyl sites of QDs. Finally, anti-ZEN mAb-QDs were stored at 4 °C for a subsequent experiment. In order to ensure the quality of the synthesis of fluorescent probes, the pH value of the synthesis and the molecular molar ratio of QDs to EDC and anti-ZEN mAb were optimized in this study.
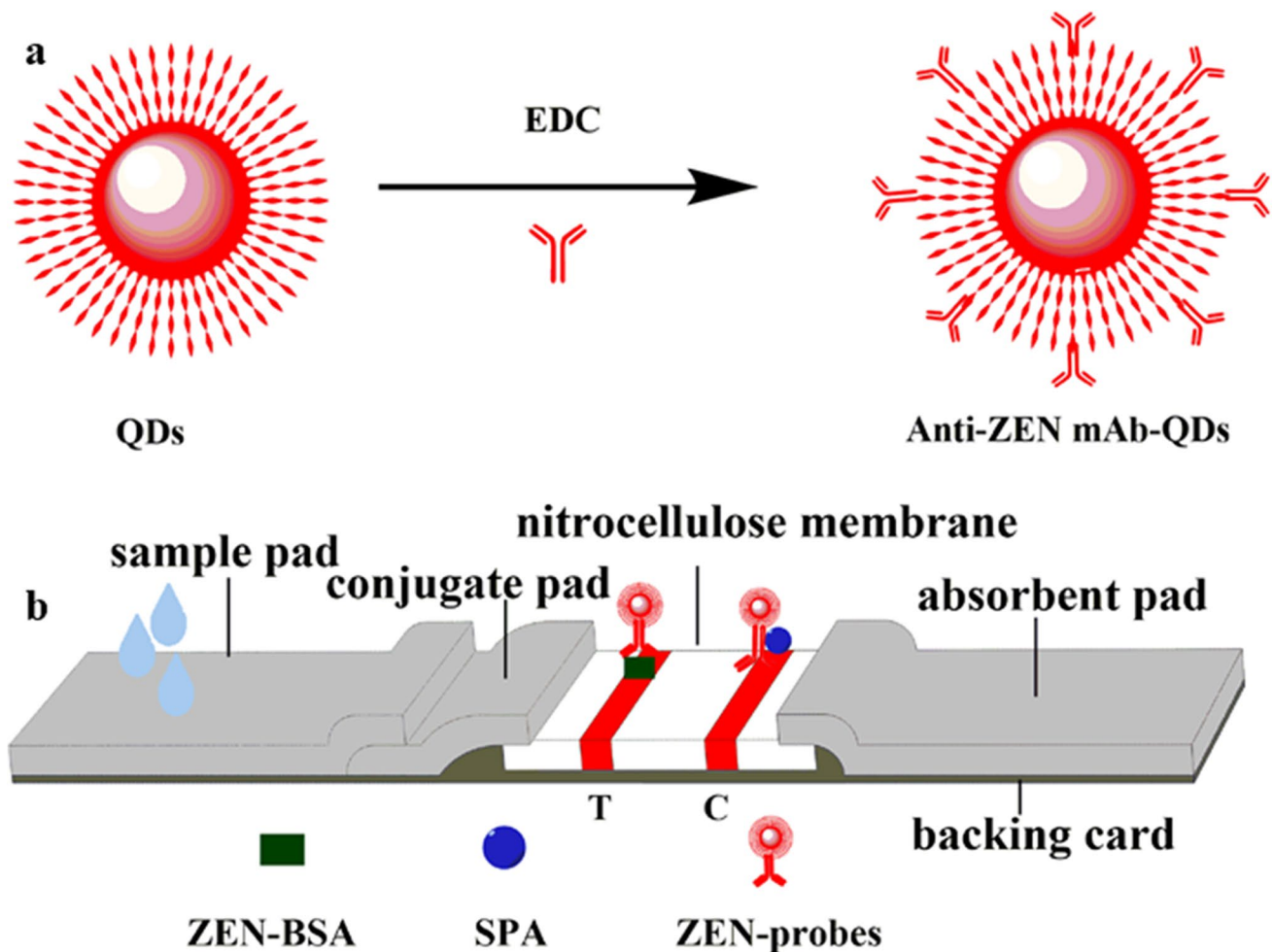
**Fig. 1** Schematic illustration of the fluorescent probes and the test strips. **a** Preparation of anti-ZEN mAb-QDs. **b** Preparation of test strips

## Evaluation of Fluorescent Probes by UV–Vis Absorption and Fluorescence Emission Spectrum

To confirm whether fluorescent probes were successfully coupled, the bioconjugation of QDs and anti-ZEN mAb was analyzed by UV–Vis absorption and fluorescence emission spectrum (Zhou et al. 2021b). The UV–vis absorption spectrum was measured by a Nanodrop 2000c Spectrophotometer. The UV–Vis application from the main menu (NanoDrop2000c Calibrator) was selected for making UV–Vis measurements. The Pedestal Option was used to carry out the measurements. The phosphate buffer solution (PBS) was used as a blank control. A 2 µL of the sample solution (QDs, anti-ZEN mAb, or fluorescent probes) was pipetted onto the bottom pedestal and measured. Sample absorbance was analyzed from 200 to 750 nm. In addition, the fluorescence spectrum was measured by a multifunctional microplate reader. The read model (fluorescence) and read type (spectrum) from the settings of SoftMax Pro v7.x were selected for making fluorescence measurements. The excitation

wavelength was set to 365 nm (ultraviolet or blue light), and the emission wavelength range was set to 450–750 nm. The wavelength step was set to 5 nm. The blank control (PBS) and samples (QDs and fluorescent probes) were automatically scanned by the SpectraMax i3X microplate reader. The data were analyzed by GraphPad Prism 8.

## Preparation of Test Strips

The test strips (Fig. 1b) were prepared according to previous research (Le et al. 2018). The SPA and ZEN-BSA solution were sprayed on nitrocellulose membrane as control line (C line) and test line (T line), respectively. The nitrocellulose membrane was dried in a drying oven for 4 h at 40 °C. Both sample and conjugate pad were pre-processed with 10 mmol/L PBS including 1.0% BSA (w/v), 0.05% trehalose (w/v), 0.25% Tween-20 (v/v), and 0.1% NaN3 (w/v), and dried immediately for 4 h at 60 °C. The test strips were assembled as follows: Firstly, a nitrocellulose membrane was attached to the base plate. Secondly, an absorbent paper was

stuck on the top of the base plate, while the conjugate pad and sample pad were sequentially attached to the bottom of the base plate, overlapping by 2 mm. Finally, the base plate was cut into strips with a width of 2.8 mm and packed into a plastic box.

## Preparation of Sample

The sample was prepared according to previous research with modification (Wang et al. 2019b). Briefly, 5.0-g corn was crushed into powder by the homogenizer. Next, 25-mL extraction buffer containing acetonitrile/water (v/v, 9/1) was added. The mixed solution was continuously vortexed for 10 min. After being filtered by filter paper, the mixed solution was centrifuged at 10,000 g for 5 min. Thereafter, 5 mL supernatant of extraction solution was dried with nitrogen and redissolved in 1 mL PBS/methanol (v/v, 19/1). Finally, the redissolved solution was diluted ninefold with PBS/methanol (v/v, 19/1) for test strip detection.

## Qualitative Detection of ZEN

The pre-treatment of corn was carried out according to the above-mentioned process. The ZEN standard was added to corn extraction for the preparation of the sample solution. The final ZEN concentrations of sample solutions were 0, 0.1, 0.5, 1, 2.5, 5, 10, 25, 50, and 100 ng/mL. The sample solutions were pipetted onto test strips. After incubating for 10 min at room temperature (25 °C), the test strips were observed with the visualization method under a UV lamp (excitation wavelength of 365 nm). The cutoff value was the lowest ZEN concentration that made the T line fluorescence invisible under a UV Lamp (Wu et al. 2019).

## Quantitative Detection of ZEN

The fluorescence intensity of T line ($FI_T$), C line ($FI_C$), and value of $FI_T/FI_C$ were recorded by a multi-channel fluorescence immunoassay analyzer. The data were analyzed and the ZEN competition inhibition curve was established by GraphPad Prism 8. The abscissa was the logarithmic value of the ZEN concentration with 10 as the base. The ordinate was the value of competition inhibition rate ($1-B/B_0$), where $B$ was the $FI_T/FI_C$ value of the test strips under different ZEN concentrations, and $B_0$ was the $FI_T/FI_C$ value of the test strips when ZEN was negative (Guo et al. 2019). The limit of detection (LOD) was calculated based on the ZEN competitive inhibition rate of 10%, and the linear detection range was calculated based on the ZEN competitive inhibition rate of 20 to 80% (Wang et al. 2019b).

## Results and Discussion

### Comprehensive Evaluation of Fluorescent Probes

The UV–Vis absorption spectrum was measured by a Nanodrop 2000c Spectrophotometer. The anti-ZEN mAb had an obvious absorption peak at 280 nm. The absorbance of anti-ZEN mAb-QDs significantly increased compared with QDs (Fig. 2a). Additionally, the fluorescence spectrum was measured by the SpectraMax i3X microplate reader. The anti-ZEN mAb-QDs and QDs possessed narrow emissions with the same emission peaks at about 610 nm (Fig. 2b). The fluorescent properties of QDs were consistent with previous reports (Guo et al. 2019; Liu et al. 2019) that QDs were suitable for the synthesis of ideal fluorescent probes. Moreover, the anti-FLE mAb-QDs were also characterized
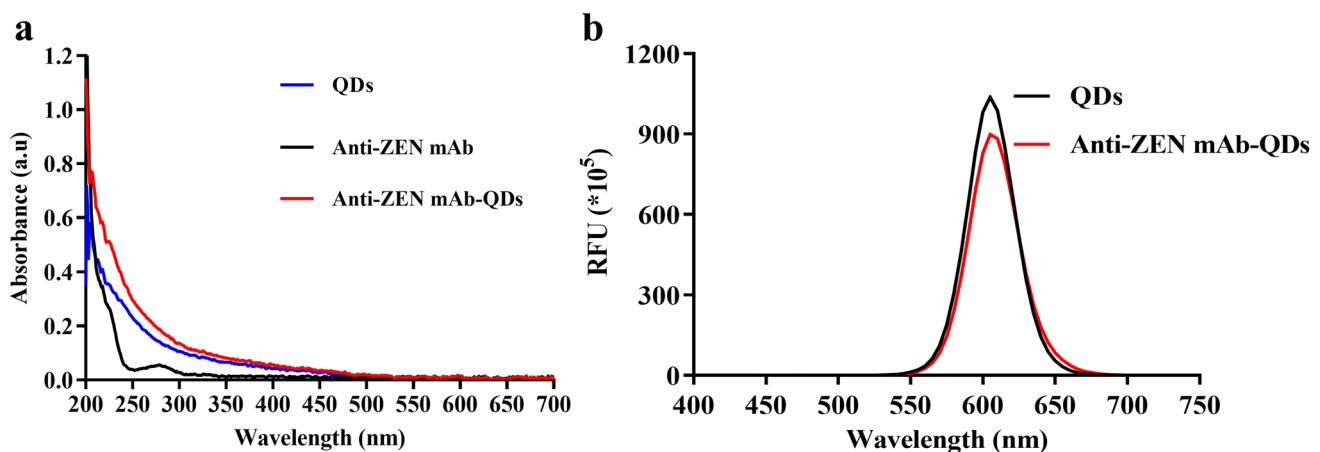


**Fig. 2** UV/Vis absorption spectrum and fluorescence emission spectrum. **a** UV/Vis absorption spectrum of QDs, anti-ZEN mAb, and anti-ZEN mAb-QDs. **b** Fluorescence emission spectrum of QDs and anti-ZEN mAb-QDs. Excitation and emission wavelengths were 365 nm and 610 nm, respectively

by agarose gel electrophoresis (Fig. 3a) and polyacrylamide gel electrophoresis (Fig. 3b). The movement rate of anti-FLE mAb-QDs was slower than that of QDs, which might be due to the increase in its molecular weight. The bioactivity of anti-ZEN mAb-QDs was characterized by the immunochromatographic assay. After adding the anti-ZEN mAb-QDs, the test strips showed red fluorescence (Fig. 3c). On the contrary, the test strips did not show red fluorescence when QDs were added. This indicated that the anti-ZEN mAb-QDs retained the bioactivity of anti-ZEN mAb, which was able to combine with SPA and ZEN-BSA. In general, the anti-ZEN mAb-QDs exhibited both the fluorescent properties of QDs and the bioactivity of anti-ZEN antibodies.

## Optimization of Bioconjugation

In order to reduce the coagulation during the coupling process and obtain more stable and sensitive fluorescent probes, the synthesis conditions were optimized in this study, including the pH value, the molar ratio of anti-ZEN monoclonal antibodies, and 1-(3-dimethylaminopropyl)-3-ethylcarbodiimide hydrochloride (EDC) (Liu et al. 2019; Wang et al. 2017). When the pH value was 7.7, the result of Fig. 4a showed that $FI_T$ and $FI_C$ were higher than other pH gradients. Figure 4b indicated that $FI_T$ and $FI_C$ reached saturated when the molar ratio of QDs to EDC was 1:125. As EDC increased, excess EDC actually reduced the value of $FI_T$. The increase in EDC molar ratio was beneficial to the binding of QDs to IgG, but an excess of EDC resulted in massive aggregation of conjugates (Song and Chan 2011). Furthermore, the amount of anti-ZEN mAb was also critical to the synthesis of fluorescent probes. Figure 4c showed that $FI_T$ and $FI_C$ reached saturated when the molar ratio of QDs to anti-ZEN mAb was 1:5. This was consistent with a previous study that each QD conjugated with 2 to 10 immunoglobulins (Liu et al. 2019). However, a higher molar ratio of mAb to QDs decreased the sensitivity of the assay (Foubert

et al. 2016; Wang et al. 2017). Therefore, the pH value of 7.7, the molar ratio of QDs to EDC (1:125), and anti-ZEN mAb (1:5) were optimization conditions in this study.

## Optimization of Test Strips

An amount of ZEN-BSA and anti-ZEN mAb-QDs was optimized with checkerboard titration, which was especially important to sensitivity and fluorescence intensity on test strips (Duan et al. 2017). The values of $FI_T$ and $FI_C$ (Table 1) were recorded by a multi-channel fluorescence immunoassay analyzer. The values of $FI_T$ and $FI_C$ increased as the concentration of ZEN-BSA increased, but decreased as the dilution factor of anti-ZEN mAb-QDs increased. The $FI_T$ and $FI_C$ reached $244 \pm 8$ a.u and $193 \pm 2$ a.u when the concentration of ZEN-BSA was 0.206 mg/mL and the probe dilution factor was 2. In addition, the ratio of $FI_T/FI_C$ was $1.262 \pm 0.044$ under optimized conditions.

## Optimization of Detection Conditions

In order to obtain a better interpretation time for detection, the immunoreaction time was optimized by test strips (Duan et al. 2017). The $FI_T$ and $FI_C$ improved continuously within 30 min (Fig. 5a). However, $FI_T/FI_C$ was relatively stable after 10 min, which indicated that 10 min was enough for detection analysis. The pH value had a slight impact on the $FI_T/FI_C$ of the test strips, but had a greater impact on the competition inhibition of the test strip. When pH was 7.4, the competition inhibition for the ZEN-spiked sample (2.5 ng/mL) reached 54% ($0.54 \pm 0.04$), which was better than several other pH values (Fig. 5b). Therefore, 0.01 mol/L PBS (pH 7.4) was chosen for this study. When the methanol concentration of the sample dilution solution increased to 5%, the competitive inhibition rate reached 47% ($0.47 \pm 0.02$). Conversely, when the methanol concentration exceeded 5%, the competition inhibition rate was significantly reduced



**Fig. 3** Characterization of QDs and anti-ZEN mAb-QDs by agarose gel electrophoresis and PAGE. 1 QDs, 2 mAb-QDs. **a** Agarose gel electrophoresis. **b** PAGE. **c** Result of original bioactivity

**a**



**b**

**c**
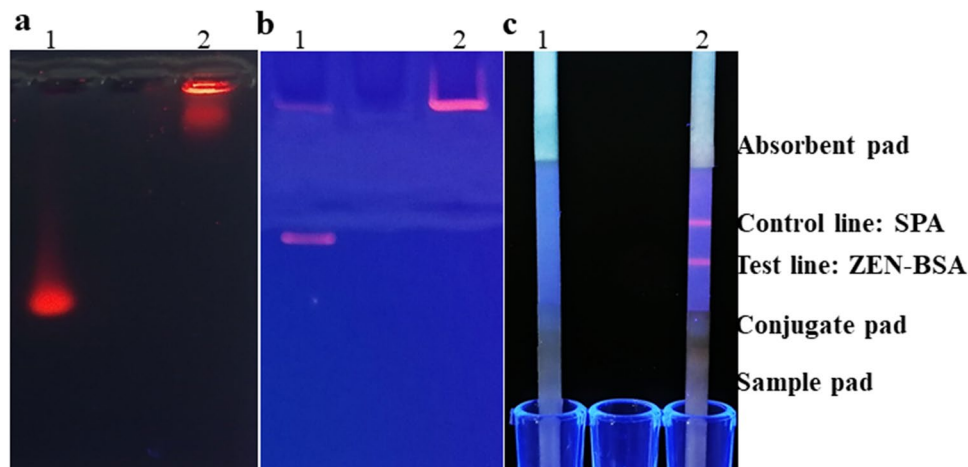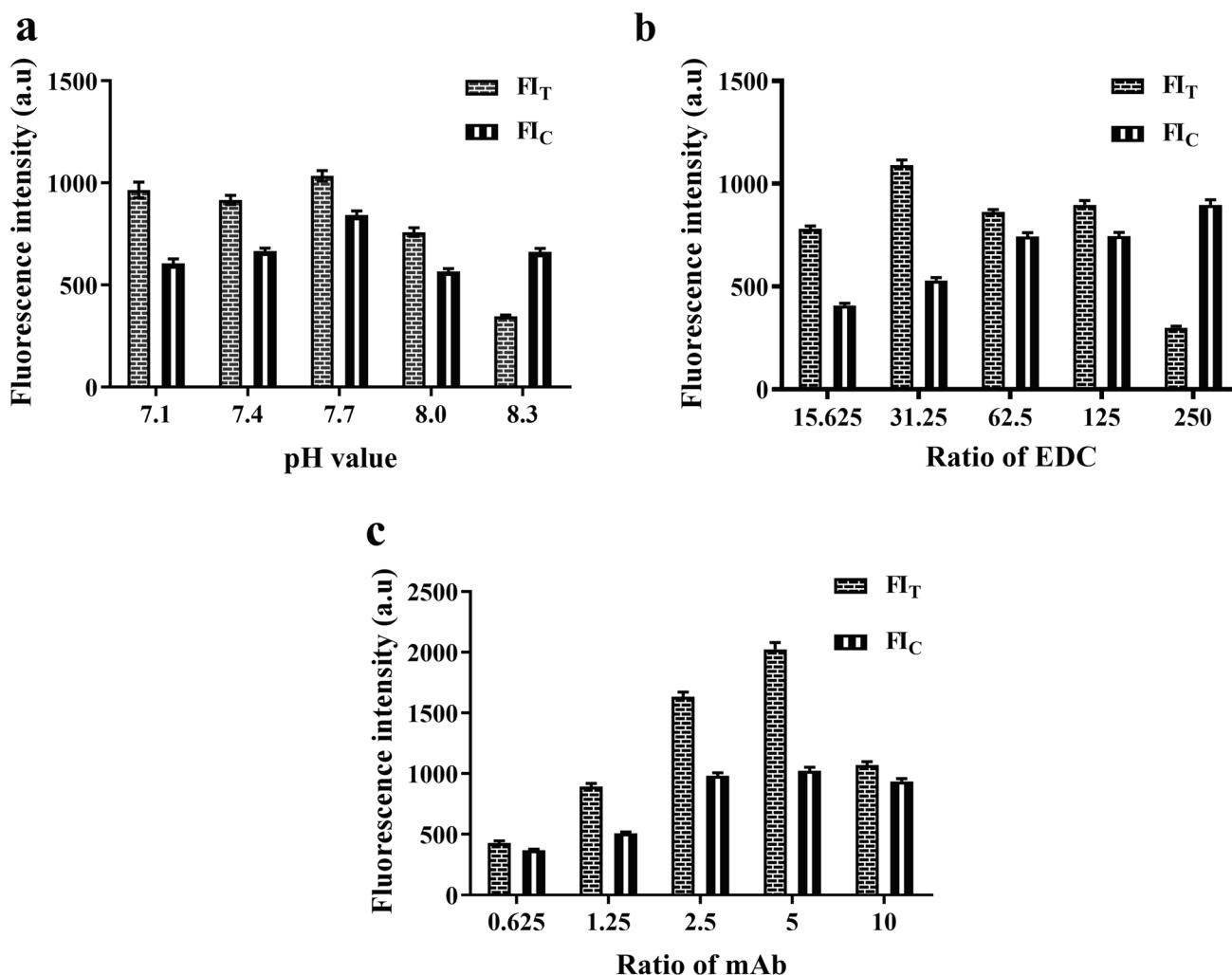
**Fig. 4** Optimization of conditions for probe synthesis. **a** The pH value of the label. **b** The amount of EDC. **c** The amount of anti-ZEN mAb

(Fig. 5c). Therefore, the optimal concentration of methanol was 5%. Previous studies also showed that the pH value and the methanol concentration influenced the analytical sensitivity of the immunochromatographic assay by affecting the immunoreaction efficiency (Shao et al. 2019; Chen et al. 2018; Xu et al. 2016). Moreover, the matrix effect was also minimized by optimizing the dilution factor of the extraction solution. The 1:9 dilution was sufficient to minimize the matrix effect. Therefore, the inhibition curve of the extraction solution (1:9 dilution) was similar to that of PBS control (Fig. 6a).

### Detection of ZEN by Test Strips

The calibration curve of ZEN was established according to the quantitative test results (Fig. 6b). The linear regression equation was $y = 0.3958x + 0.3233$ ($R^2 = 0.9914$). The LOD and 50% comparative inhibition concentration

($IC_{50}$) were 0.273 ng/mL and 2.792 ng/mL, respectively. Furthermore, the test strips had a wide detection range of 0.488–15.996 ng/mL. Under the irradiation of ultraviolet light (excitation wavelength of 365 nm), the T line fluorescence was invisible when the ZEN-spiked concentration was 10 ng/mL (Fig. 7).

### Performance of Test Strips

Briefly, DON, T-2, OTA, OTC, and OTD were tested by test strips with a concentration of 1000 ng/mL. The $FI_T/FI_C$ was consistent with the PBS control, except that the $FI_T/FI_C$ was significantly reduced when detecting ZEN by test strips (Fig. 6c). The result indicated that the test strips had good specificity and negligible cross-reactivity (CR) with other mycotoxins.

The recovery assay is one of the principal methods for the study of accuracy (Gonzalez et al. 1999). Therefore, the

**Table 1** Optimization of the concentration of ZEN-BSA and the dilution of fluorescent probes by using a checkerboard titration ($n=3$)

| No | Concentration ZEN-BSA (mg/mL) | Dilution of fluorescent probes | $FI_T$ | $FI_C$ | $FI_T/FI_C$ (B)[a] |
|---|---|---|---|---|---|
| 1 | 1.65 | 2 | $939 \pm 15$ | $329 \pm 3$ | $2.858 \pm 0.052$ |
| 2 | 1.65 | 4 | $504 \pm 60$ | $172 \pm 18$ | $2.923 \pm 0.052$ |
| 3 | 1.65 | 8 | $293 \pm 52$ | $102 \pm 19$ | $2.875 \pm 0.091$ |
| 4 | 0.825 | 2 | $730 \pm 27$ | $319 \pm 16$ | $2.288 \pm 0.040$ |
| 5 | 0.825 | 4 | $464 \pm 36$ | $190 \pm 19$ | $2.447 \pm 0.067$ |
| 6 | 0.825 | 8 | $185 \pm 5$ | $74 \pm 5$ | $2.493 \pm 0.180$ |
| 7 | 0.412 | 2 | $472 \pm 59$ | $266 \pm 42$ | $1.785 \pm 0.060$ |
| 8 | 0.412 | 4 | $274 \pm 16$ | $154 \pm 13$ | $1.782 \pm 0.051$ |
| 9 | 0.412 | 8 | $135 \pm 3$ | $78 \pm 5$ | $1.722 \pm 0.084$ |
| 10 | 0.206 | 2 | $244 \pm 8$ | $193 \pm 2$ | $1.262 \pm 0.044$ |
| 11 | 0.206 | 4 | $157 \pm 2$ | $125 \pm 3$ | $1.257 \pm 0.015$ |
| 12 | 0.206 | 8 | $87 \pm 7$ | $74 \pm 8$ | $1.175 \pm 0.027$ |

[a]$B$ was value of $FI_T/FI_C$

ZEN-spiked recovery was performed for validation purposes according to previous research (Shao et al. 2019). Procedures based on spiked samples were presented in this study. Briefly, uncontaminated corn was previously added ZEN standard, which the final concentration was 2.5, 5, and 10 ng/mL in the spiked sample. Each spiked sample was prepared in three replicates for precision analyses of intra-assay and inter-assay. In the intra-assay, recoveries ranged from 85.62 to 98.57%, and the coefficient of variation (CV) was less than 5.53%; in the inter-assay, recoveries ranged from 84.43 to 100.54%, and the CV was less than 8.79% (Table 2). Therefore, the recoveries and CV showed that the test strips had good accuracy and precision.

## Conclusion

This study assessed the efficacy of the QD immunochromatographic test strip to monitor and control ZEN residues in corn. The fluorescence probes (anti-ZEN mAb-QDs) exhibited both the fluorescent properties of QDs and the
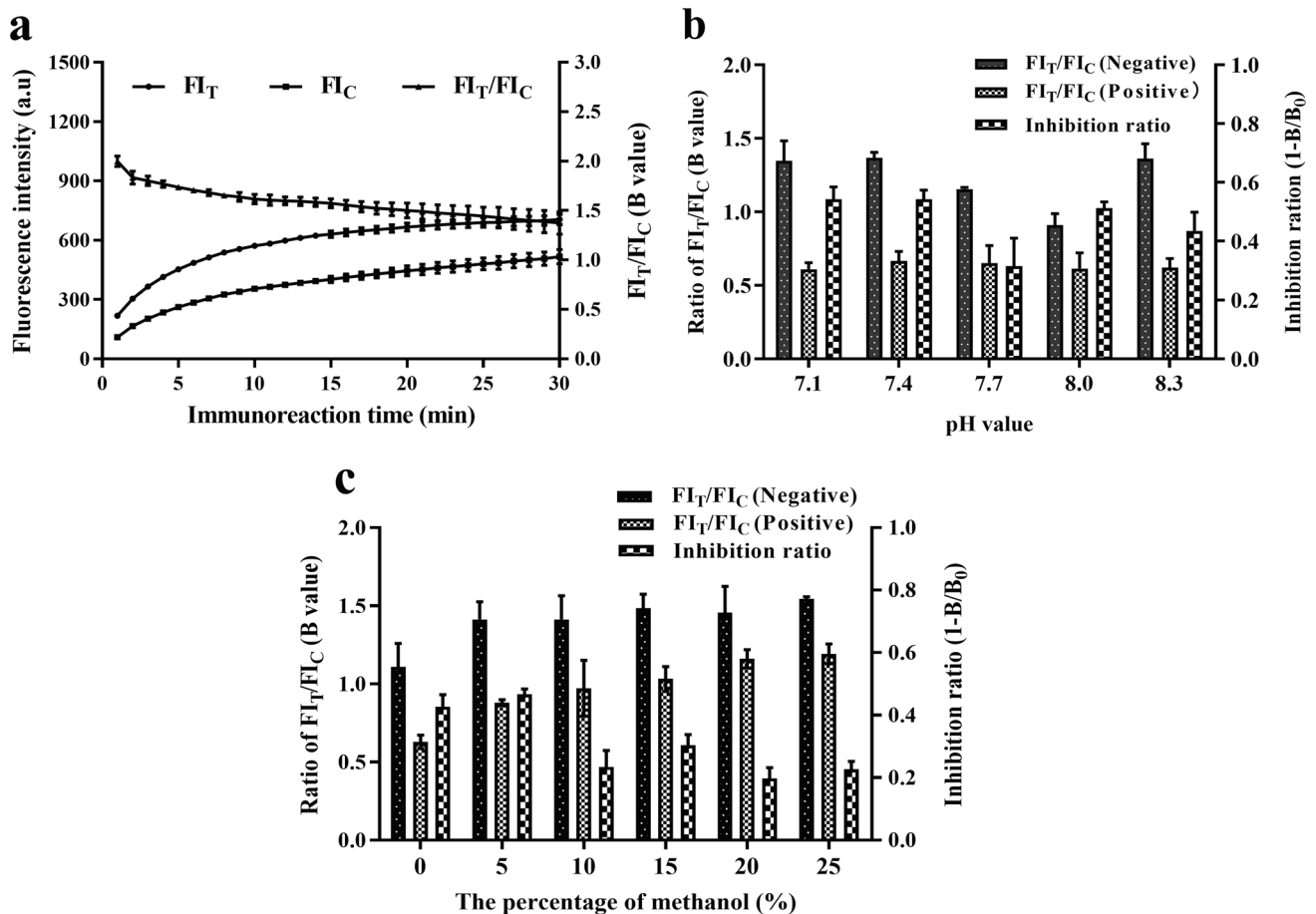


**Fig. 5** Optimization detection conditions of the test strips. **a** The reaction time for the test strips. **b** The pH value of the sample solution. **c** The influence of the methanol concentration in the sample solution
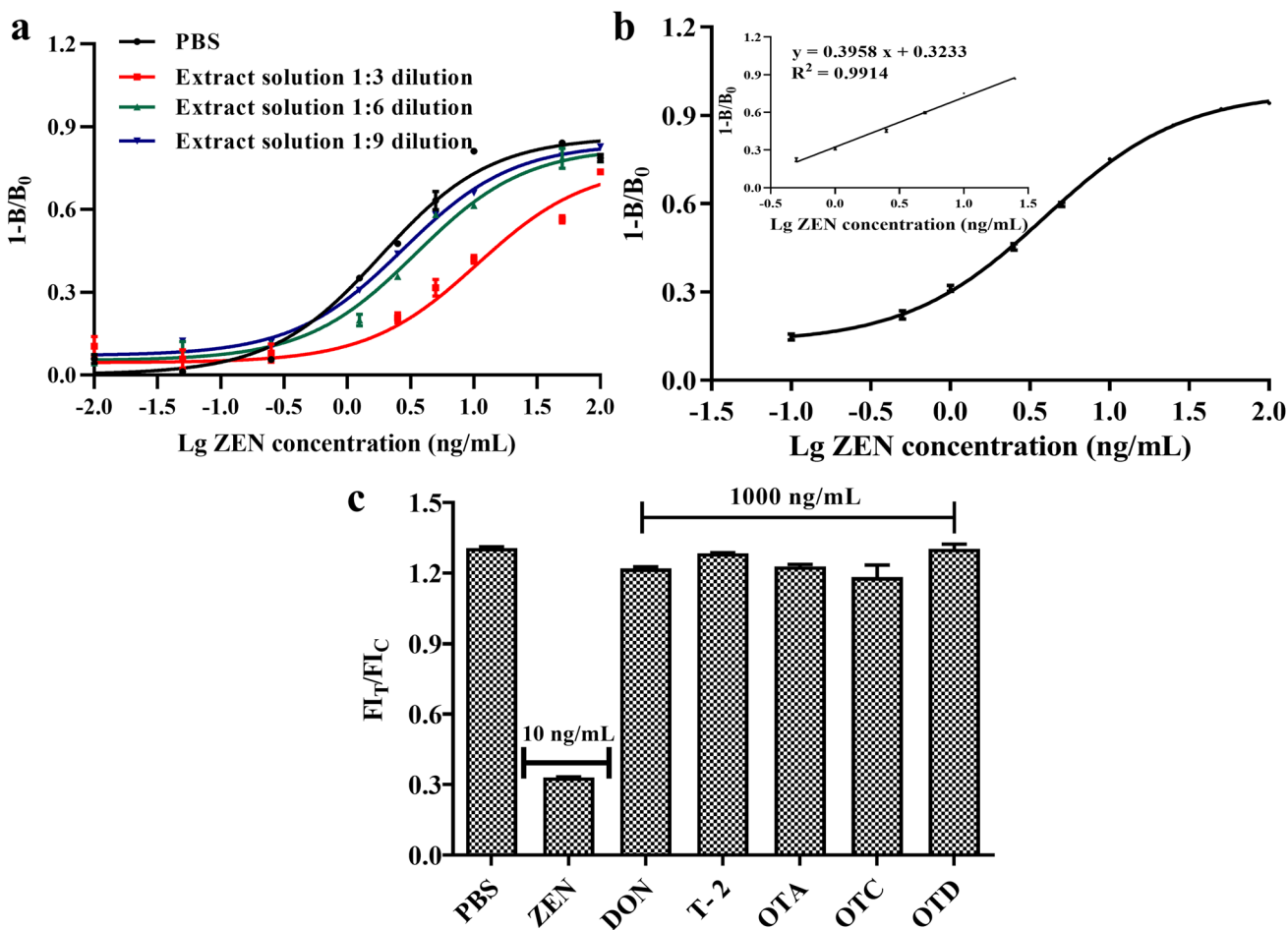
**Fig. 6** Evaluation of the test strips. **a** Matrix influences of sample solution. **b** The relationship between the concentration of ZEN and competitive inhibition rate. Inset: the standard curve. **c** Specificity of test strips. The concentration of DON, T-2, OTA, OTC, and OTD was 1000 ng/mL and the ZEN 10 ng/mL

**Fig. 7** Qualitative detection of ZEN with visual observation under the irradiation of ultraviolet light (excitation wavelength: 365 nm)
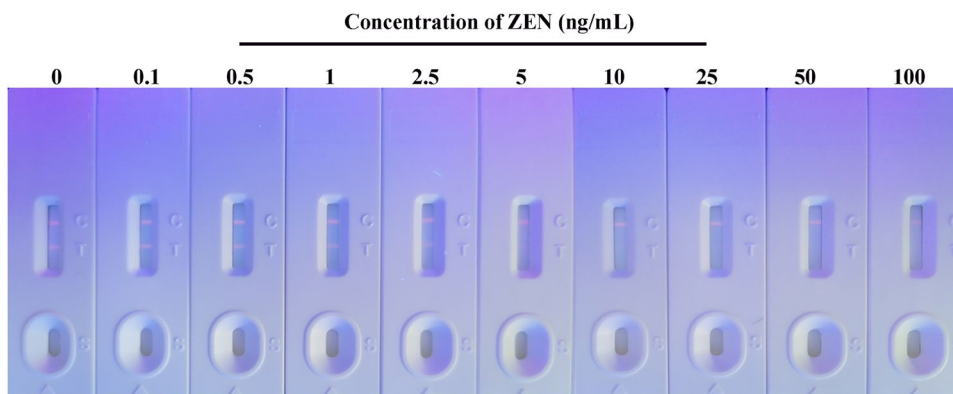


bioactivity of anti-ZEN antibodies. To improve the performance of the developed test strips, the interpretation time, the pH value, and the methanol concentration were optimized. Under optimized conditions, the test strips were used in the qualitative and quantitative detection of ZEN, and its specificity, accuracy, and precision were confirmed. Overall, the test strips were favored the detection of ZEN in corn, which was significant to point-of-care detection of mycotoxins.

**Table 2** Accuracy and precision of the QD immunochromatographic test strip

| Spiked ZEN (ng/mL) | Intra-assay | | | Inter-assay[b] | | |
| --- | --- | --- | --- | --- | --- | --- |
| | Test[a] | Recovery (%) | CV (%) | Test[a] | Recovery (%) | CV (%) |
| 10 | 9.01±0.17 | 90.11±1.70 | 1.89 | 9.06±0.64 | 90.63±6.41 | 7.07 |
| 5 | 4.93±0.16 | 98.57±3.39 | 3.44 | 5.03±0.44 | 100.54±8.84 | 8.79 |
| 2.5 | 2.14±0.12 | 85.62±4.73 | 5.53 | 2.11±0.11 | 84.43±4.44 | 5.26 |

[a] Mean value of three replicates at each ZEN-spiked concentration

[b] Assay was completed every 1 day for 3 days continuously

**Data Availability** All data generated or analyzed during this study are included in this published article.

## Declarations

**Ethics Approval** All the authors declare that no human participants and animals were involved in this study.

**Informed Consent** Informed consent is not applicable.

**Conflict of Interest** The authors declare no competing interests.

## References

Alshannaq A, Yu JH (2017) Occurrence, toxicity, and analysis of major mycotoxins in food. Int J Environ Res Public Health 14(6):1–20. https://doi.org/10.3390/ijerph14060632

Beloglazova NV, Goryacheva IY, Niessner R, Knopp D (2011) A comparison of horseradish peroxidase, gold nanoparticles and qantum dots as labels in non-instrumental gel-based immunoassay. Microchim Acta 175(3–4):361–367. https://doi.org/10.1007/s00604-011-0682-4

Cha SH, Kim SH, Bischoff K, Kim HJ, Son SW, Kang HG (2012) Production of a highly group-specific monoclonal antibody against zearalenone and its application in an enzyme-linked immunosorbent assay. J Vet Sci 13(2):119–125. https://doi.org/10.4142/jvs.2012.13.2.119

Chen XR, Liang Y, Zhang WJ, Leng YK, Xiong YH (2018) A colorimetric immunoassay based on glucose oxidase-induced AuNP aggregation for the detection of fumonisin B-1. Talanta 186:29–35. https://doi.org/10.1016/j.talanta.2018.04.018

Chen Y, Fu QQ, Xie J, Wang H, Tang Y (2019) Development of a high sensitivity quantum dot-based fluorescent quenching lateral flow assay for the detection of zearalenone. Anal Bioanal Chem 411(10):2169–2175. https://doi.org/10.1007/s00216-019-01652-1

Duan H, Huang X, Shao Y, Zheng L, Guo L, Xiong Y (2017) Size-dependent immunochromatographic assay with quantum dot nanobeads for sensitive and quantitative detection of ochratoxin A in corn. Anal Chem 89(13):7062–7068. https://doi.org/10.1021/acs.analchem.7b00869

Foubert A, Beloglazova NV, De Saeger S (2017) Comparative study of colloidal gold and quantum dots as labels for multiplex screening tests for multi-mycotoxin detection. Anal Chim Acta 955:48–57. https://doi.org/10.1016/j.aca.2016.11.042

Foubert A, Beloglazova NV, Rajkovic A, Sas B, Madder A, Goryacheva IY, De Saeger S (2016) Bioconjugation of quantum dots: review & impact on future application. Trac-Trend Anal Chem 83:31–48. https://doi.org/10.1016/j.trac.2016.07.008

Gao XH, Chan WCW, Nie SM (2002) Quantum-dot nanocrystals for ultrasensitive biological labeling and multicolor optical encoding. J Biomed Opt 7(4):532–537. https://doi.org/10.1117/1.1506706

Gonzalez AG, Herrador MA, Asuero AG (1999) Intra-laboratory testing of method accuracy from recovery assays. Talanta 48(3):729–736. https://doi.org/10.1016/s0039-9140(98)00271-9

Guo L, Shao Y, Duan H, Ma W, Leng Y, Huang X, Xiong Y (2019) Magnetic quantum dot nanobead-based fluorescent immunochromatographic assay for the highly sensitive detection of aflatoxin B1 in dark soy sauce. Anal Chem 91(7):4727–4734. https://doi.org/10.1021/acs.analchem.9b00223

Huang XL, Aguilar ZP, Xu HY, Lai WH, Xiong YH (2016) Membrane-based lateral flow immunochromatographic strip with nanoparticles as reporters for detection: a review. Biosens Bioelectron 75:166–180. https://doi.org/10.1016/j.bios.2015.08.032

Kolosova AY, De Saeger S, Sibanda L, Verheijen R, Van Peteghem C (2007) Development of a colloidal gold-based lateral-flow immunoassay for the rapid simultaneous detection of zearalenone and deoxynivalenol. Anal Bioanal Chem 389(7–8):2103–2107. https://doi.org/10.1007/s00216-007-1642-z

Krska R, Josephs R (2001) The state-of-the-art in the analysis of estrogenic mycotoxins in cereals. Fresenius J Anal Chem 369(6):469–476. https://doi.org/10.1007/s002160100715

Le T, Zhang ZH, Wu J, Shi HX, Cao XD (2018) A fluorescent immunochromatographic strip test using a quantum dot-antibody probe for rapid and quantitative detection of 1-aminohydantoin in edible animal tissues. Anal Bioanal Chem 410(2):565–572. https://doi.org/10.1007/s00216-017-0756-1

Li RX, Meng CZ, Wen Y, Fu W, He PL (2019) Fluorometric lateral flow immunoassay for simultaneous determination of three mycotoxins (aflatoxin B-1, zearalenone and deoxynivalenol) using quantum dot microbeads. Microchim Acta 186(12):748. https://doi.org/10.1007/s00604-019-3879-6

Liu Y, Zhao Y, Zhang T, Chang Y, Wang S, Zou R, Zhu G, Shen L, Guo Y (2019) Quantum dots-based immunochromatographic strip for rapid and sensitive detection of acetamiprid in agricultural products. Front Chem 7:76. https://doi.org/10.3389/fchem.2019.00076

Liu Z, Hua Q, Wang J, Liang Z, Li J, Wu J, Shen X, Lei H, Li X (2020) A smartphone-based dual detection mode device integrated with two lateral flow immunoassays for multiplex mycotoxins in cereals. Biosens Bioelectron 158:112178. https://doi.org/10.1016/j.bios.2020.112178

Luo Y, Liu XJ, Li JK (2018) Updating techniques on controlling mycotoxins - a review. Food Control 89:123–132. https://doi.org/10.1016/j.foodcont.2018.01.016

Mahmoudi T, de la Guardia M, Shirdel B, Mokhtarzadeh A, Baradaran B (2019) Recent advancements in structural improvements of lateral flow assays towards point-of-care testing. Trac-Trends Anal Chem 116:13–30. https://doi.org/10.1016/j.trac.2019.04.016

Massart F, Meucci V, Saggese G, Soldani G (2008) High growth rate of girls with precocious puberty exposed to estrogenic mycotoxins. J Pediatr 152(5):690–695. https://doi.org/10.1016/j.jpeds.2007.10.020

Sajid M, Kawde AN, Daud M (2015) Designs, formats and applications of lateral flow assay: a literature review. J Saudi Chem Soc 19(6):689–705. https://doi.org/10.1016/j.jscs.2014.09.001

Shao Y, Duan H, Guo L, Leng Y, Lai W, Xiong Y (2018) Quantum dot nanobead-based multiplexed immunochromatographic assay for simultaneous detection of aflatoxin B1 and zearalenone. Anal Chim Acta 1025:163–171. https://doi.org/10.1016/j.aca.2018.03.041

Shao Y, Duan H, Zhou S, Ma T, Guo L, Huang X, Xiong Y (2019) Biotin-streptavidin system-mediated ratiometric multiplex immunochromatographic assay for simultaneous and accurate quantification of three mycotoxins. J Agric Food Chem 67(32):9022–9031. https://doi.org/10.1021/acs.jafc.9b03222

Song F, Chan WC (2011) Principles of conjugating quantum dots to proteins via carbodiimide chemistry. Nanotechnology 22(49):494006. https://doi.org/10.1088/0957-4484/22/49/494006

Sun YN, Xing GX, Yang JF, Wang FY, Deng RG, Zhang GP, Hu XF, Zhang Y (2016) Development of an immunochromatographic test strip for simultaneous qualitative and quantitative detection of ochratoxin A and zearalenone in cereal. J Sci Food Agric 96(11):3673–3678. https://doi.org/10.1002/jsfa.7550

Taranova NA, Berlina AN, Zherdev AV, Dzantiev BB (2015) 'Traffic light' immunochromatographic test based on multicolor quantum dots for the simultaneous detection of several antibiotics in milk. Biosens Bioelectron 63:255–261. https://doi.org/10.1016/j.bios.2014.07.049

Thongrussamee T, Kuzmina NS, Shim WB, Jiratpong T, Eremin SA, Intrasook J, Chung DH (2008) Monoclonal-based enzyme-linked immunosorbent assay for the detection of zearalenone in cereals. Food Addit Contam Part A Chem Anal Control Expo Risk Assess 25(8):997–1006. https://doi.org/10.1080/02652030701823159

Ugarte I, Serrano IC, Palomares E, Pacios R (2012) Quantum dots as a light indicator for emitting diodes and biological coding. In. Quantum dots - a variety of new applications, pp 115–134

Wang Q, Jing JY, Wang BT (2019a) Highly sensitive SPR biosensor based on graphene oxide and staphylococcal protein A co-modified TFBG for human IgG detection. Ieee T Instrum Meas 68(9):3350–3357. https://doi.org/10.1109/Tim.2018.2875961

Wang S, Liu Y, Jiao S, Zhao Y, Guo Y, Wang M, Zhu G (2017) Quantum-dot-based lateral flow immunoassay for detection of neonicotinoid residues in tea leaves. J Agric Food Chem 65(46):10107–10114. https://doi.org/10.1021/acs.jafc.7b03981

Wang Y, Xu J, Qiu Y, Li P, Liu B, Yang L, Barnych B, Hammock BD, Zhang C (2019b) Highly specific monoclonal antibody and sensitive quantum dot beads-based fluorescence immunochromatographic test strip for tebuconazole assay in Agricultural products. J Agric Food Chem 67(32):9096–9103. https://doi.org/10.1021/acs.jafc.9b02832

Wu JK, Ma JW, Wang H, Qin DM, An L, Ma Y, Zheng ZT, Hua XD, Wang TL, Wu XJ (2019) Rapid and visual detection of benzothiostrobin residue in strawberry using quantum dot-based lateral flow test strip. Sensor Actuat B-Chem 283:222–229. https://doi.org/10.1016/j.snb.2018.11.137

Xu P, Li J, Huang XL, Duan H, Ji YW, Xiong YH (2016) Effect of the tip length of multi-branched AuNFs on the detection performance of immunochromatographic assays. Anal Methods-Uk 8(16):3316–3324. https://doi.org/10.1039/c5ay03274a

Xu Y, Ma B, Chen EJ, Yu XP, Ye ZH, Sun CX, Zhang MZ (2021) Dual fluorescent immunochromatographic assay for simultaneous quantitative detection of citrinin and zearalenone in corn samples. Food Chem 336. https://doi.org/10.1016/j.foodchem.2020.127713

Zhang DH, Li PW, Zhang Q, Zhang W (2011) Ultrasensitive nano-gold probe-based immunochromatographic assay for simultaneous detection of total aflatoxins in peanuts. Biosens Bioelectron 26(6):2877–2882. https://doi.org/10.1016/j.bios.2010.11.031

Zhang J, Sun Y, Wu Q, Zhang H, Bai Y, Song D (2013) A protein A modified Au-graphene oxide composite as an enhanced sensing platform for SPR-based immunoassay. Analyst 138(23):7175–7181. https://doi.org/10.1039/c3an01553j

Zhang X, Eremin SA, Wen K, Yu X, Li C, Ke Y, Jiang H, Shen J, Wang Z (2017) Fluorescence polarization immunoassay based on a new monoclonal antibody for the detection of the zearalenone class of mycotoxins in maize. J Agric Food Chem 65(10):2240–2247. https://doi.org/10.1021/acs.jafc.6b05614

Zhang Z, Hu X, Zhang Q, Li P (2016) Determination for multiple mycotoxins in agricultural products using HPLC-MS/MS via a multiple antibody immunoaffinity column. J Chromatogr B Analyt Technol Biomed Life Sci 1021:145–152. https://doi.org/10.1016/j.jchromb.2016.02.035

Zhao H, Chen X, Shen C, Qu B (2017) Determination of 16 mycotoxins in vegetable oils using a QuEChERS method combined with high-performance liquid chromatography-tandem mass spectrometry. Food Addit Contam Part A Chem Anal Control Expo Risk Assess 34(2):255–264. https://doi.org/10.1080/19440049.2016.1266096

Zhou J, Liu Z, Yang Q, Qian W, Chen Y, Qi Y, Wang A (2021a) Multiple fluorescence immunoassay for the simultaneous detection of Zearalenone and Ochratoxin A. Anal Biochem 628:114288. https://doi.org/10.1016/j.ab.2021.114288

Zhou J, Yang Q, Liang C, Chen Y, Zhang X, Liu Z, Wang A (2021b) Detection of ochratoxin A by quantum dots-based fluorescent immunochromatographic assay. Anal Bioanal Chem 413(1):183–192. https://doi.org/10.1007/s00216-020-02990-1

**Publisher's Note** Springer Nature remains neutral with regard to jurisdictional claims in published maps and institutional affiliations.